# Kinetics and Thermodynamics of Restricted Rotation of the Formyl Group in Nitrobenzaldehyde Anion Radicals

**Mario Branca,[†] Aldo Gamba,[†] Mario Barzaghi,[‡] and Massimo Simonetta*[‡]**

*Contribution from the Institute of Physical Chemistry, University of Sassari, 07100 Sassari, Italy, and C.N.R. Center for "Study of Structure/Reactivity Relations" and Institute of Physical Chemistry, University of Milan, 20133 Milano, Italy.* *Received November 12, 1981*

**Abstract:** The barrier to rotation about the carbonyl carbon-phenyl carbon bond of 3-nitrobenzaldehyde anion radical in *N,N*-dimethylformamide solution has been determined by a detailed line-shape analysis of the corresponding electron paramagnetic resonance (EPR) spectra at different temperatures. At 25 °C the cis conformation is favored by 0.98 kcal mol$^{-1}$ in free energy, and the free-energy barrier to the cis-trans conversion amounts to 9.35 kcal mol$^{-1}$. Both enthalpy and entropy contributions to the free-energy profile are accurately evaluated ($\Delta H^{\ddagger}$ = 3.91, $\Delta H^{\circ}$ = -1.13 kcal mol$^{-1}$; $\Delta S^{\ddagger}$ = -18.2, $\Delta S^{\circ}$ = -7.1 cal mol$^{-1}$ K$^{-1}$). The effects of ionic association and solvation on the barrier are discussed. The EPR spectra of 4-nitrobenzaldehyde and 2-nitrobenzaldehyde anion radicals are also reported as a function of temperature. In these cases, the barriers to internal rotation are too high to be surmounted on the EPR time scale. STO-3G ab initio MO calculations are given for benzaldehyde, 3-nitrobenzaldehyde, 4-nitrobenzaldehyde, and the corresponding anion radicals. The spin distribution in the anion radicals is calculated by McLachlan and INDO methods.

## Introduction

Barriers to rotation about the carbonyl carbon-phenyl carbon bond in aryl aldehydes and ketones have been a long-standing subject of spectroscopic investigations.[1-4] Recent experimental and theoretical studies of substituted benzaldehydes and acetophenones point out an active interest in these systems.[5,6]

In the course of our investigations on the anion radicals of aromatic nitro derivatives,[7-14] the determination of the activation parameters of intra- and intermolecular dynamic processes involving the anion radicals was already encountered.[8,10,11,13] In particular, the barrier to internal rotation of the amido group about the benzene-to-carbonyl bond of the three isomers of nitrobenzamide was predicted by the combined use of electron paramagnetic resonance (EPR) spectroscopy and theoretical calculations.[11]

In this paper we investigate by dynamic EPR spectroscopy the hindered internal rotation of the formyl group of 3-nitrobenzaldehyde (3-NBA) anion radical, for which no experimental dynamic data are available. In addition, complementary experimental results are presented for the anion radicals of the ortho and para isomers of nitrobenzaldehyde, which have been previously investigated by EPR spectroscopy.[3,15,16] The comparison is interesting as the carbonyl group can be sensitive to electronic disturbance of the nitro group at various sites in the aromatic ring, because of its ability to enter into conjugation with the adjacent system. In particular, it should provide a better understanding of the mechanism of internal rotation for the three isomers in terms of mesomeric, inductive, and steric contributions to the isomerization process. In view of this, comparison of the barrier heights of the anion radicals and the corresponding parent compounds should also be of interest. In reality, the introduction of an unpaired electron into the $\pi$ system of nitrobenzaldehyde should cause an increase in the height of the barrier, by better stabilizing the coplanar ground state through resonance effects. On the contrary, specific solvation of the nitro group or complexation of the nitro group by alkali metal cations is expected to cause a decrease in the height of the barrier, by driving both spin and charge density from the carbonyl group and the benzene ring to the nitro group, and be destabilizing the coplanar ground state. On the basis of these considerations, we extended the investigation to the effects of ionic association and solvation on the barrier height.

Particular attention was devoted to the analysis of spectral data, by checking the accuracy and the reliability of the computational methods and models used through a quantitative evaluation of the agreement between experimental and calculated spectra based on error analysis. This procedure ensures a confident evaluation of random errors affecting the determination of the thermodynamic parameters which govern internal rotation. It is well known that activation enthalpies ($\Delta H^{\ddagger}$), unlike free energies ($\Delta G^{\ddagger}$), are prone to systematic errors.[17-19] It has been suggested regularly in the last 15 years in the literature that the entropy of activation of first-order processes associated with rotational isomerization is likely to be near zero.[19] However, a clear confirmation of noticeable entropy contributions due, for example, to the existence of differential solvation effects would certainly be of interest. In this view, the risk of errors can be attenuated by a combined use of a large range of active temperatures and a total line-shape analysis, especially where more complex, and therefore "more sensitive", spectra are concerned.[17]

Finally, in order to gain more insight both on the equilibrium conformations and the details of the isomerization process, we used quantum mechanical models at ab initio levels of approximation to explore the potential energy surface for intermolecular rearrangement in nitrobenzaldehydes and their anion radicals.

[†] University of Sassari.
[‡] University of Milan.

(1) Sternhell, S. In "Dynamic Nuclear Magnetic Resonance Spectroscopy"; Cotton, F. A., Jackman, L. M., Eds.; Academic Press: New York, 1975; pp 163-201.
(2) Kaminski, W. *Z. Naturforsch., A* **1970**, *25*, 639.
(3) Kaminski, W. Mobius, K. *J. Magn. Reson.* **1971**, *5*, 182.
(4) (a) Sommer, J. M.; Jost, R. P.; Drakenberg, T. *J. Magn. Reson.* **1976**, *21*, 93. (b) Drakenberg, T.; Jost, R.; Sommer, J. *Ibid.* **1976**, *8*, 579. (c) Barthelemy, J. F.; Jost, R.; Sommer, J. *Ibid.* **1978**, *11*, 438, 443.
(5) Antypas, W. G., Jr.; Sinkola, L. V. M.; Kleier, D. A. *J. Org. Chem.* **1981**, *46*, 1172.
(6) St. Amour, T. E.; Burgar, M. I.; Valentine, B.; Fiat, D. *J. Am. Chem. Soc.* **1981**, *103*, 1128.
(7) Barzaghi, M.; Beltrame, P. L.; Gamba, A.; Simonetta, M. *J. Am. Chem. Soc.* **1978**, *100*, 251.
(8) Barzaghi, M.; Cremaschi, P.; Gamba, A.; Morosi, G.; Oliva, C.; Simonetta, M. *J. Am. Chem. Soc.* **1978**, *100*, 3132.
(9) Barzaghi, M.; Gamba, A.; Morosi, G.; Simonetta, M. *J. Phys. Chem.* **1978**, *82*, 2105.
(10) Barzaghi, M.; Oliva, C.; Simonettta, M. *J. Phys. Chem.* **1980**, *84*, 1717.
(11) Barzaghi, M.; Oliva, C.; Simonetta, M. *J. Phys. Chem.* **1980**, *84*, 1959.
(12) Barzaghi, M.; Oliva, C.; Gamba, A.; Saba, A. *J. Chem. Soc., Perkin Trans. 2* **1980**, 1617.
(13) Barzaghi, M.; Oliva, C.; Simonetta, M. *J. Phys. Chem.* **1981**, *85*, 1799.
(14) Branca, M.; Gamba, A.; Saba, A.; Barzaghi, M.; Simonetta, M. *J. Chem. Soc., Perkin Trans. 2* **1982**, 349.
(15) Rieger, P. H.; Fraenkel, G. K. *J. Chem. Phys.* **1962**, *37*, 2811.
(16) Stone, E.; Maki, A. H. *J. Chem. Phys.* **1963**, *38*, 1999.
(17) Binsch, G. In ref 1, pp 45-81.
(18) Anet, F. A. L.; Anet, R. In ref 1, pp 543-619.
(19) Martin, M. L.; Mabon, F.; Trierweller, M. *J. Phys. Chem.* **1981**, *85*, 76.

0002-7863/82/1504-6506$01.25/0 

Table I. Experimental and Calculated Hfs Constants (G) for Magnetic Nuclei in the 3-NBA Anion Radicals

| nucleus | ring position | exptl[a] cis ⇄ trans[b] | exptl[a] cis[c] | exptl[a] trans[c,d] | McLachlan cis | McLachlan trans | INDO cis | INDO trans |
|---|---|---|---|---|---|---|---|---|
| H(CHO) | 1 | *f* | *f* | *f* | −0.15 | −0.02 | −0.35 | −0.30 |
| H | 2 | 2.927 ± 0.006 | 2.734 ± 0.007 | 3.432 ± 0.010 | −2.18 | −2.84 | −2.49 | −2.50 |
| $N(NO_2)$ | 3 | 8.502 ± 0.005 | 8.414 ± 0.006 | 8.961 ± 0.011 | 8.79 | 9.25 | 9.53 | 9.60 |
| H | 4 | 3.925 ± 0.007 | 4.213 ± 0.006 | 3.432 ± 0.010 | −4.63 | −4.18 | −2.81 | −2.78 |
| H | 5 | 1.109 ± 0.004 | 1.142 ± 0.006 | 1.020 ± 0.012 | 1.43 | 1.37 | 1.32 | 1.30 |
| H | 6 | 4.659 ± 0.007 | 4.894 ± 0.006 | 4.146 ± 0.011 | −5.06 | −4.63 | −2.65 | −2.61 |
| populations | | | 0.72 ± 0.06 | 0.28 ± 0.06 | | | | |

[a] Electrolytic reduction in DMF containing TBAP as a supporting electrolyte. [b] Averaged hfs constants at 25 °C. [c] At −50 °C. [d] The spectrum of the trans isomer is shifted 0.139 ± 0.005 G downfield with respect to the spectrum of the cis isomer. [f] Unresolved hfs constant.

## Experimental Section

2-, 3-, and 4-nitrobenzaldehydes (Aldrich) were sublimated before use. Anion radicals were generated both by controlled-potential electrolysis in *N,N*-dimethylformamide (DMF), dimethyl sulfoxide ($Me_2SO$), an 80:20 solution of $Me_2SO$ and *tert*-butyl alcohol (*t*-BuOH), methanol, and water, using tetra-*n*-butylammonium perchlorate (TBAP) as supporting electrolyte, and by chemical reduction in DMF with sodium methoxide. Attempts to obtain the alkali metals ion pairs of 3-NBA and 4-NBA in tetrahydrofuran (THF) and 1,2-dimethoxyethane failed, owing to the high reactivity of the compounds in these media. Only 2-NBA gave stable ion pairs by reduction on sodium mirror in THF. The sample preparation, experimental procedures, and spectrometer system employed in this study have been described in previous papers.[7-13]

Hyperfine splitting (hfs) constants and other relevant parameters, such as rate constants, line width, and contributions to line width from isotropic and/or anisotropic modulation of hfs constants, have been obtained through an iterative least-squares line-shape fitting procedure. The iterative least-squares program EPR80 was used to perform the analysis of the dynamic EPR spectra. Details on the computer program EPR80 have been discussed elsewhere,[13] and only the essential points will be covered here.

In the fast motional region, for each allowed transition λ, the following line-width expression was used:

$$W_\lambda = 2.3^{-1/2}|\gamma_e|^{-1}(T_2^{-1})_\lambda = W_{\text{relax},\lambda} + W_{\text{exch},\lambda} \quad (1)$$

where $W_{\text{relax},\lambda}$ gives the contribution to relaxation broadening by anisotropic dipolar modulation through the well-known relationship:[20,21]

$$W_{\text{relax},\lambda} = A + \sum_\alpha B_\alpha \bar{M}_{\lambda\alpha} + \sum_\alpha C_\alpha \eta(M_{\lambda\alpha}) + \sum_{\alpha<\beta} E_{\alpha\beta} M_{\lambda\alpha} M_{\lambda\beta} \quad (2)$$

The line-width contribution $W_{\text{exch},\lambda}$ produced by the modulation of isotropic hfs constants, has been expressed as:[20]

$$W_{\text{exch},\lambda} = \sum_{\alpha\le\beta} F_{\alpha\beta} M_{\lambda\alpha} M_{\lambda\beta} \quad (3)$$

In the slow exchange region, calculations were afforded by the static model or the general density matrix method. In Figure 1, the *R* factor[22] for the experimental spectra of 3-NBA anion radical is plotted as a function of temperature. The *R* factor is a measure of goodness of fit and it has proved to be a very useful error criterion when fits of different spectra and/or different models are to be compared. When the fast exchange model (eq 1-3) is applied, the *R* factor shows a flat minimum between 80 and 25 °C and increases steeply at temperatures lower than 25 °C. Indeed, the region between 25 and 15 °C corresponds to the coalescence temperatures of the hfs constants. As coalescence temperatures cannot accurately be derived from complex spectra by simple inspection, the *R* factor can be used as a tool to recognize promptly the breakdown of the fast exchange model. In the same way the plot of *R* vs. *T* indicates that the "static" model can be applied at temperatures lower than −40 °C. In the intermediate region (i.e., from +20 to −40 °C), the general density matrix method should be applied. A rise of *R* factor at temperatures higher than 80 °C reflects a loss of spectral resolution. The experimental spectra were digitized "by hand" over ~300 data points. The digitized spectra were than processed by our program EPR80 on a Univac 1100/80. The calculated spectra were displayed by a CALCOMP plotter. A few results of the procedure outlined above are shown in Tables I-IV and in Figures 2-4.

The hfs constants, line-width coefficients, rate constants, and their standard errors were entered to a weighted linear least-squares program for the analysis of their temperature dependence, as described in the next sections. Particular care was devoted to check the sample temperature, and in some cases the temperatures given by the automatic apparatus were checked by a thermocouple inserted in the sample.

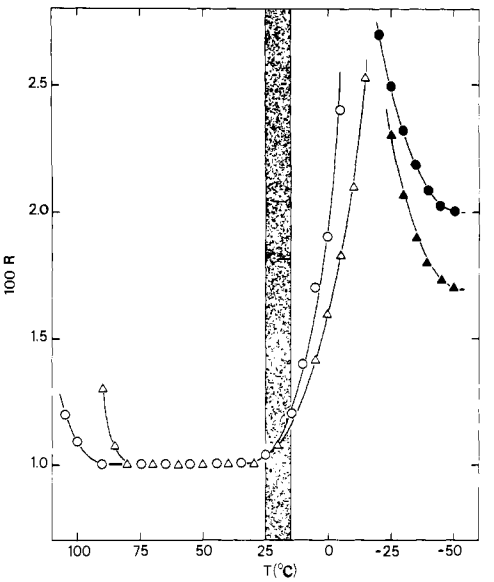


**Figure 1.** Plot of *R* factor as a function of temperature for the EPR spectra of 3-NBA anion radical in DMF, obtained by electrolytic reduction (circles) and by chemical reduction with $CH_3ONa$ (triangles). Open symbols, fast motional model; blackened symbols, static model. The darkened region corresponds to the coalescence temperature of the hfs constants.

Table II. Experimental and Calculated Hfs Constants (G) for Magnetic Nuclei in the 4-NBA and 2-NBA Anion Radicals at −20 °C

| benzaldehyde | nucleus | ring position | exptl[a] | McLachlan[b,c] | INDO[b] |
|---|---|---|---|---|---|
| 4-$NO_2$ | H(CHO) | 1 | 1.363 ± 0.002 | −1.54 | 0.57 |
| | H | 2 | 0.256 ± 0.001 | 0.26 | 1.24 |
| | H | 3 | 2.296 ± 0.002 | −2.38 | −2.50 |
| | $N(NO_2)$ | 4 | 5.216 ± 0.001 | 6.48 | 8.00 |
| | H | 5 | 2.993 ± 0.002 | −2.75 | −2.51 |
| | H | 6 | 0.397 ± 0.001 | 0.33 | 1.24 |
| 2-$NO_2$ | H(CHO) | 1 | 0.951 ± 0.003 | −1.37 | 1.80 |
| | $N(NO_2)$ | 2 | 6.795 ± 0.002 | 7.09 | 9.98 |
| | H | 3 | 2.275 ± 0.002 | −2.11 | −2.07 |
| | H | 4 | 0.384 ± 0.002 | 0.31 | 1.12 |
| | H | 5 | 3.442 ± 0.002 | −3.34 | −1.90 |
| | H | 6 | 0.607 ± 0.002 | 1.13 | 1.27 |

[a] Electrolytic reduction in DMF containing TBAP as a supporting electrolyte, at −20 °C. [b] 6-C is the ring carbon atom nearest to the carbonyl oxygen atom. [c] For 2-$NBA^{-\cdot}$ the best results are obtained with $k_{C_1\text{-}C_\alpha} = 0.725 = 0.78 \cos(21.5)$.

## Spin Density Calculations

Spin density calculations were carried out by means of the McLachlan method,[23] based on the $\sigma/\pi$ approximation, and by means of the INDO method,[24] which includes all valence electrons. The α and β integrals

(20) Freed, J. H.; Fraenkel, G. K. *J. Chem. Phys.* **1963**, *39*, 326.
(21) Muus, L. T.; Atkins, P. W., Eds. "Electron Spin Relaxation in Liquids"; Plenum Press: New York, 1975.
(22) Hamilton, W. C. *Acta Crystallogr.* **1965**, *18*, 502.
(23) McLachlan, A. D. *Mol. Phys.* **1960**, *3*, 233.

Table III. Line-Width Contributions (G) of the Internal Rotation for 3-NBA$^{-\cdot}$ in DMF (Counterion TBA) as a Function of Temperature (°C)

| $T$ | $F_{NN}$ | $F_{N6}$ | $F_{N4}$ | $F_{N2}$ | $F_{N5}$ | $W_0$ |
|---|---|---|---|---|---|---|
| 105 | 0.010 ± 0.005 | −0.019 ± 0.006 | −0.021 ± 0.006 | 0.020 ± 0.007 | | 0.274 ± 0.006 |
| 100 | 0.011 ± 0.005 | −0.022 ± 0.006 | −0.024 ± 0.007 | 0.023 ± 0.008 | | 0.285 ± 0.007 |
| 90 | 0.015 ± 0.004 | −0.029 ± 0.005 | −0.030 ± 0.006 | 0.033 ± 0.007 | | 0.286 ± 0.005 |
| 80 | 0.019 ± 0.005 | −0.037 ± 0.007 | −0.039 ± 0.008 | 0.038 ± 0.009 | | 0.286 ± 0.007 |
| 70 | 0.025 ± 0.004 | −0.048 ± 0.005 | −0.050 ± 0.006 | 0.048 ± 0.007 | | 0.287 ± 0.005 |
| 65 | 0.026 ± 0.005 | −0.056 ± 0.006 | −0.053 ± 0.006 | 0.056 ± 0.008 | | 0.287 ± 0.005 |
| 60 | 0.033 ± 0.005 | −0.065 ± 0.006 | −0.074 ± 0.007 | 0.061 ± 0.008 | | 0.294 ± 0.005 |
| 55 | 0.039 ± 0.005 | −0.081 ± 0.006 | −0.088 ± 0.007 | 0.072 ± 0.009 | −0.011 ± 0.006 | 0.294 ± 0.005 |
| 45 | 0.041 ± 0.006 | −0.098 ± 0.008 | −0.100 ± 0.009 | 0.084 ± 0.011 | −0.014 ± 0.008 | 0.323 ± 0.007 |
| 35 | 0.089 ± 0.005 | −0.154 ± 0.007 | −0.165 ± 0.008 | 0.157 ± 0.010 | −0.018 ± 0.006 | 0.330 ± 0.005 |
| 25 | 0.099 ± 0.008 | −0.213 ± 0.014 | −0.231 ± 0.014 | 0.205 ± 0.016 | −0.027 ± 0.009 | 0.389 ± 0.008 |
| 15 | 0.143 ± 0.010 | −0.303 ± 0.018 | −0.327 ± 0.018 | 0.296 ± 0.020 | −0.034 ± 0.008 | 0.404 ± 0.008 |
| 10 | 0.189 ± 0.016 | −0.394 ± 0.030 | −0.425 ± 0.030 | 0.380 ± 0.031 | −0.046 ± 0.010 | 0.439 ± 0.011 |
| 5 | 0.221 ± 0.022 | −0.462 ± 0.044 | −0.506 ± 0.044 | 0.450 ± 0.045 | −0.054 ± 0.012 | 0.472 ± 0.015 |
| 0 | 0.273 ± 0.036 | −0.578 ± 0.072 | −0.634 ± 0.073 | 0.562 ± 0.073 | −0.068 ± 0.015 | 0.519 ± 0.023 |
| −5 | 0.314 ± 0.055 | −0.663 ± 0.110 | −0.751 ± 0.111 | 0.671 ± 0.111 | −0.069 ± 0.020 | 0.563 ± 0.033 |
| | $F_{64}$ | $F_{62}$ | $F_{65}$ | $F_{42}$ | $F_{45}$ | $F_{25}$ |
| 105 | 0.030 ± 0.011 | −0.028 ± 0.012 | | −0.031 ± 0.011 | | |
| 100 | 0.029 ± 0.013 | −0.032 ± 0.012 | | −0.035 ± 0.010 | | |
| 90 | 0.040 ± 0.040 | −0.039 ± 0.010 | | −0.043 ± 0.009 | 0.010 ± 0.008 | |
| 80 | 0.052 ± 0.015 | −0.049 ± 0.013 | | −0.055 ± 0.010 | 0.012 ± 0.010 | |
| 70 | 0.067 ± 0.008 | −0.063 ± 0.010 | | −0.070 ± 0.010 | 0.015 ± 0.009 | |
| 65 | 0.079 ± 0.009 | −0.072 ± 0.012 | | −0.080 ± 0.011 | 0.017 ± 0.010 | |
| 60 | 0.093 ± 0.009 | −0.082 ± 0.011 | | −0.091 ± 0.010 | 0.019 ± 0.009 | |
| 55 | 0.096 ± 0.009 | −0.094 ± 0.011 | 0.011 ± 0.010 | −0.105 ± 0.011 | 0.021 ± 0.010 | −0.019 ± 0.008 |
| 45 | 0.146 ± 0.012 | −0.114 ± 0.015 | 0.015 ± 0.013 | −0.140 ± 0.014 | 0.027 ± 0.012 | −0.023 ± 0.010 |
| 35 | 0.180 ± 0.010 | −0.174 ± 0.011 | 0.020 ± 0.009 | −0.192 ± 0.011 | 0.035 ± 0.009 | −0.030 ± 0.007 |
| 35 | 0.292 ± 0.017 | −0.242 ± 0.018 | 0.027 ± 0.014 | −0.260 ± 0.018 | 0.046 ± 0.014 | −0.038 ± 0.011 |
| 15 | 0.387 ± 0.021 | −0.340 ± 0.022 | 0.038 ± 0.013 | −0.364 ± 0.021 | 0.062 ± 0.013 | −0.048 ± 0.011 |
| 10 | 0.491 ± 0.033 | −0.418 ± 0.033 | 0.046 ± 0.015 | −0.456 ± 0.032 | 0.066 ± 0.016 | −0.059 ± 0.013 |
| 5 | 0.588 ± 0.048 | −0.506 ± 0.048 | 0.060 ± 0.018 | −0.554 ± 0.047 | 0.080 ± 0.020 | −0.060 ± 0.016 |
| 0 | 0.717 ± 0.077 | −0.622 ± 0.076 | 0.069 ± 0.022 | −0.684 ± 0.076 | 0.105 ± 0.026 | −0.092 ± 0.020 |
| −5 | 0.819 ± 0.116 | −0.712 ± 0.116 | 0.078 ± 0.028 | −0.849 ± 0.116 | 0.116 ± 0.035 | −0.080 ± 0.027 |

Table IV. Hfs Constants ($a_\alpha$, gauss), Line-Width Contributions ($F_{\alpha\alpha}$, gauss), Rate Constants, and Activation Free Energies of Internal Rotation for 3-NBA$^{-\cdot}$ in Different Solvents (Counterion TBA) at 25 °C

| solvent | $a_N$ | $a_{6\text{-H}}$ | $a_{4\text{-H}}$ | $a_{2\text{-H}}$ | $a_{5\text{-H}}$ |
|---|---|---|---|---|---|
| $H_2O$ | 13.976 ± 0.003 | 3.585 ± 0.004 | 3.585 ± 0.004 | 3.585 ± 0.004 | 1.172 ± 0.005 |
| $CH_3OH$ | 12.311 ± 0.002 | 3.990 ± 0.003 | 3.668 ± 0.002 | 3.376 ± 0.003 | 1.156 ± 0.003 |
| $Me_2SO$/*t*-BuOH | 9.505 ± 0.003 | 4.606 ± 0.003 | 3.963 ± 0.003 | 3.120 ± 0.003 | 1.139 ± 0.002 |
| $Me_2SO$ | 9.113 ± 0.004 | 4.702 ± 0.005 | 4.014 ± 0.005 | 3.053 ± 0.005 | 1.135 ± 0.004 |
| DMF | 8.502 ± 0.005 | 4.659 ± 0.007 | 3.925 ± 0.007 | 2.927 ± 0.006 | 1.109 ± 0.004 |
| solvent | $F_{NN}$ | $F_{66}$ | $F_{44}$ | $F_{22}$ | $F_{55}$ |
| $H_2O$ | 0.0 | 0.0 | 0.0 | 0.0 | 0.0 |
| $CH_3OH$ | 0.018 ± 0.001 | 0.068 ± 0.004 | 0.092 ± 0.005 | 0.144 ± 0.008 | 0.000 ± 0.000 |
| $Me_2SO$/*t*-BuOH | 0.099 ± 0.007 | 0.042 ± 0.004 | 0.123 ± 0.011 | 0.108 ± 0.010 | 0.001 ± 0.001 |
| $Me_2SO$ | 0.132 ± 0.006 | 0.205 ± 0.010 | 0.262 ± 0.013 | 0.251 ± 0.012 | 0.007 ± 0.001 |
| DMF | 0.136 ± 0.006 | 0.264 ± 0.012 | 0.317 ± 0.014 | 0.231 ± 0.011 | 0.000 ± 0.001 |

| solvent | $10^7 k_{obsd}$, s$^{-1}$ | $\Delta G^\ddagger$, kcal mol$^{-1}$ |
|---|---|---|
| $H_2O$ | | |
| $CH_3OH$ | 31.8 ± 1.4 | 5.33 ± 0.02 |
| $Me_2SO$/*t*-BuOH | 5.7 ± 0.3 | 6.29 ± 0.03 |
| $Me_2SO$ | 4.3 ± 0.2 | 6.47 ± 0.02 |
| DMF | 4.0 ± 0.1 | 7.08 ± 0.01 |

required by the McLachlan method were inferred from the literature ($\alpha_i = \alpha_0 + h_i\beta_0$; $h_C = 0.0$; $h_{N\cdot} = 2.2$ $h_{O\cdot} = 1.4$; $\beta_{ij} = k_{ij}\beta$; $k_{C\text{-}C} = 1.0$; $k_{C\text{-}N\cdot} = 1.2$; $k_{C\text{-}O\cdot} = 1.6$; $k_{N\cdot\text{-}O\cdot} = 1.67$). The exchange integral for the benzene-to-carbonyl bond was measured $0.78\beta_0$. A small increase ($h_{C'} = -0.1$) in the value of the Coulomb integral of the ring carbon atom (C′) nearest to the carbonyl oxygen atom was introduced to account for the asymmetry of the spin distribution around the carbonyl group.[15] Hfs constants were obtained from McLachlan spin densities through usual McConnell-type relationship ($a_H = -24.734\rho_C$ and $a_{N(NO_2)} = 32.951(2\rho_N - \rho_O)$).[7] Model geometries were assumed for INDO calculations, as described in the next section. Careful choice of a suitable geometry is compulsory in order to describe correctly the competitive effects of the CHO and $NO_2$ groups on the spin density distribution of nitrobenzaldehyde anion radicals. For example, the electron-withdrawing power of the formyl group is greatly overestimated with respect to the electron-withdrawing power of the nitro group when the geometry proposed by Pople and co-workers is used.[25] In Tables I and II the results of McLachlan and INDO calculations are compared with the experimental values. The McLachlan method gives a more satisfactory interpretation of the experimental spin distribution than the INDO method. In particular, the McLachlan method better reproduces both the differences of hfs constants in the two rotation isomers of 3-NBA$^{-\cdot}$, and the difference in the ortho and meta hydrogen hfs constants of 4-NBA$^{-\cdot}$. However, both methods reproduce identical assignments of hfs constants. The only exception is found for 2-NBA$^{-\cdot}$, where the McLachlan calculation yields $|a(5\text{-H})| > |a(3\text{-H})|$, while the reverse order is predicted by the INDO method.

(24) Dobosh, P. A. *QCPE* **1969**, *11*, 141.

(25) Pople, J. A.; Beveridge, D. L.; Dobosh, P. A. *J. Am. Chem. Soc.* **1968**, *80*, 4201.

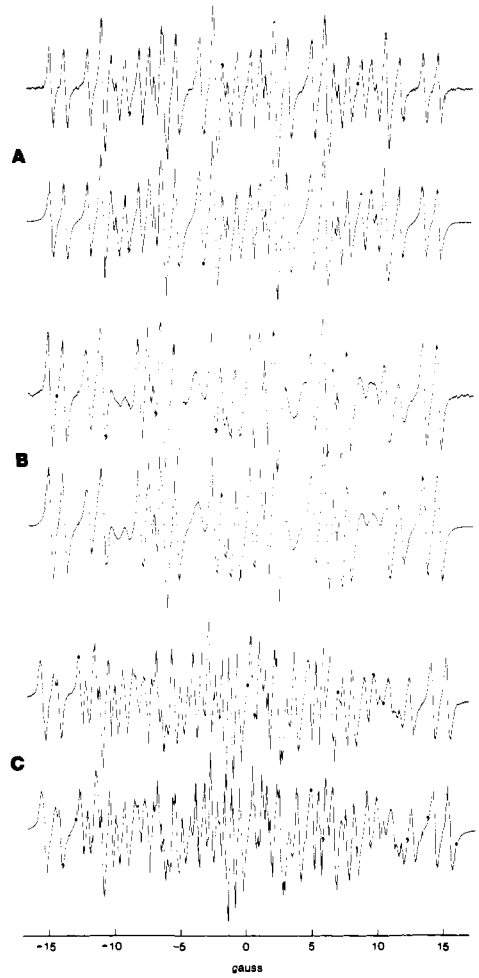


**Figure 2.** EPR spectra of 3-NBA$^{-\cdot}$ in DMF (counterion TBA) at different temperatures. In each case, the upper trace is the experimental spectrum; the lower trace is a matched computer-synthesized spectrum. (A) $T$ = 105 °C; $\bar{a}$ = 8.466 ± 0.003, $\bar{a}_N$ = 4.671 ± 0.005, $\bar{a}_H$ = 3.928 ± 0.006, $\bar{a}_H$ = 2.885 ± 0.005, $\bar{a}_H$ = 1.100 ± 0.004, $A$ = 0.282 ± 0.006 G and the $F$'s reported in Table III; $R$ = 0.012. (B) $T$ = 15 °C; $\bar{a}_N$ = 8.515 ± 0.004, $\bar{a}_H$ = 4.654 ± 0.006, $\bar{a}$ = 3.923 ± 0.006, $\bar{a}_H$ = 2.939 ± 0.006, $\bar{a}_H$ = 1.104 ± 0.004, $A$ = 0.404 ± 0.008 G and the $F$'s reported in Table III; $R$ = 0.012. (C) $T$ = −50 °C; the hfs constants and the equilibrium populations of the two isomers are reported in Table I; $A_{cis}$ = 0.338 ± 0.005, $A_{trans}$ = 0.312 ± 0.005, $B_{N,cis}$ = $B_{N,trans}$ = 0.063 ± 0.008, $C_{N,cis}$ = $C_{N,trans}$ = 0.103 ± 0.008 G; $H_{cis}$ − $H_{trans}$ = 0.137 ± 0.005 G; $R$ = 0.020.

## Calculations of the Barriers to Internal Rotation

Barriers to the rigid rotation of the formyl group were determined both by an ab initio SCF-MO calculation using a STO-3G basis set[26,27] and INDO[24] MO methods. The geometry of 2-NBA is known from X-ray[28] and neutron diffraction[29] data. For the remaining compounds we assumed an idealized geometry, modeled from that of 2-NBA: hexagonal benzene ring with C–C, 1.381 Å; C–H, 1.08 Å; ∠C–C–C, 120°; bond lengths and angles of carbonyl and nitro groups as in 2-NBA; the nitro group coplanar with the ring and bisecting the external ring angle. The INDO torsional energy minima of both 3-NBA radical anion and its parent compound correspond to a dihedral angle of 90° for the rigid rotation of the formyl group about the benzene-to-carbonyl bond. These unreliable results are in accordance with the failure of the CNDO/2 method to predict the barriers and the conformations in benzaldehyde and other conjugated systems.[30] Therefore, we neglect INDO results in discussing the equilibrium conformations of nitrobenzaldehydes. In table V the results of ab initio MO calculations are compared with the experimental values. These data will be discussed in the next sections.

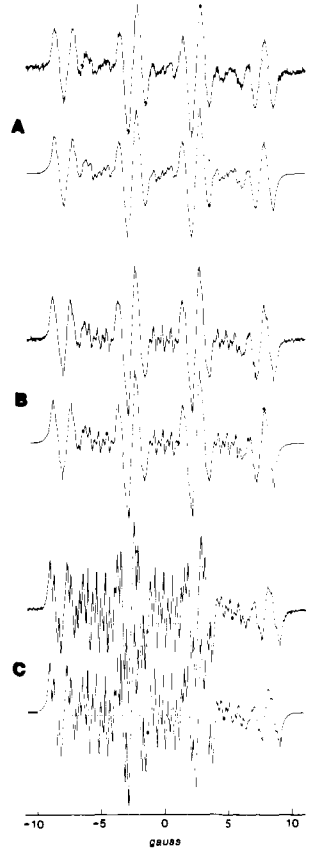


**Figure 3.** EPR spectra of 4-NBA$^{-\cdot}$ in DMF (counterion TBA) at different temperatures. In each case, the upper trace is the experimental spectrum; the lower trace is a matched computer-synthesized spectrum. (A) $T$ = 105 °C; $a_N$ = 4.986 ± 0.003, $a_H$ = 2.871 ± 0.005, $a_H$ = 2.213 ± 0.004, $a_H$ = 1.383 ± 0.003, $a_H$ = 0.361 ± 0.002, $a_H$ = 0.210 ± 0.003, $A$ = 0.313 ± 0.001 G; $R$ = 0.009. (B) $T$ = 60 °C; $a_N$ = 5.066 ± 0.002, $a_H$ = 2.916 ± 0.003, $a_H$ = 2.233 ± 0.003, $a_H$ = 1.371 ± 0.002, $a_H$ = 0.373 ± 0.001, $a_H$ = 0.221 ± 0.002, $A$ = 0.287 ± 0.004 G; $R$ = 0.007. (C) $T$ = −40 °C; $a_N$ = 5.273 ± 0.002, $a_H$ = 3.013 ± 0.003, $a_H$ = 2.309 ± 0.003, $a_H$ = 1.357 ± 0.002, $a_H$ = 0.405 ± 0.002, $a_H$ = 0.263 ± 0.002, $A$ = 0.220 ± 0.003, $B_N$ = 0.046 ± 0.004, $C_N$ = 0.044 ± 0.005 G; $R$ = 0.011.

## Rotational Isomerism of 3-NBA Anion Radical: Experimental Results

The EPR spectra of 3-NBA anion radical, obtained by controlled-potential electrolysis in DMF containing TBAP (0.1 M) were recorded in the range from −50 to 105 °C. TBAP was used as supporting electrolyte as its large cation prevents the formation of tight ion pairs. Significant changes of line shapes were found on temperature variation. Above 5 °C, a very strong line-width alternation is observed in the hyperfine patterns (Figure 2B), indicating a modulation of isotropic couplings. Below 20 °C, the hfs patterns of two different paramagnetic species are easily recognized (Figure 2C), as the splittings from two forms, although of comparable magnitude, are significantly different. Furthermore, the centers of the two spectra are split by 0.139 ± 0.005 G at −50 °C, giving for the difference in spectroscopic splitting factors the value $\Delta G = 8.6 \times 10^{-5}$.

These facts can be explained by restricted rotation of the formyl group with a frequency comparable to the difference in the hfs constants of the two possible rotation isomers. When the conversion rate is small enough on the EPR time scale ($T \leq -20$ °C),

(26) Hehre, W. J.; Stewart, R. F.; Pople, J. A. *J. Chem. Phys.* **1969**, *51*, 2657.
(27) Cremaschi, P.; Morosi, G.; Palmieri, P. MILAN: a computer program for ab initio calculations using s, p, and d GTO's.
(28) Coppens, P.; Schmidt, G. M. *Acta Crystallogr.* **1964**, *17*, 222.
(29) Coppens, P. *Acta Crystallogr.* **1964**, *17*, 573.
(30) (a) Gropen, O.; Seip, H. M. *Chem. Phys. Lett.* **1971**, *11*, 445. (b) Hoffmann, R.; Swenson, J. R. *J. Phys. Chem.* **1970**, *74*, 415.
(31) Drakenberg, G.; Jost, R.; Sommer, J. *J. Chem. Soc., Chem. Commun.* **1974**, 1011.
(32) Anet, F. A. L.; Ahmad, M. *J. Am. Chem. Soc.* **1964**, *86*, 119.
(33) Lunazzi, L. *Tetrahedron Lett.* **1975**, 1205.
(34) Hehre, W. J.; Radom, L.; Pople, J. A. *J. Am. Chem. Soc.* **1972**, *94*, 1496.

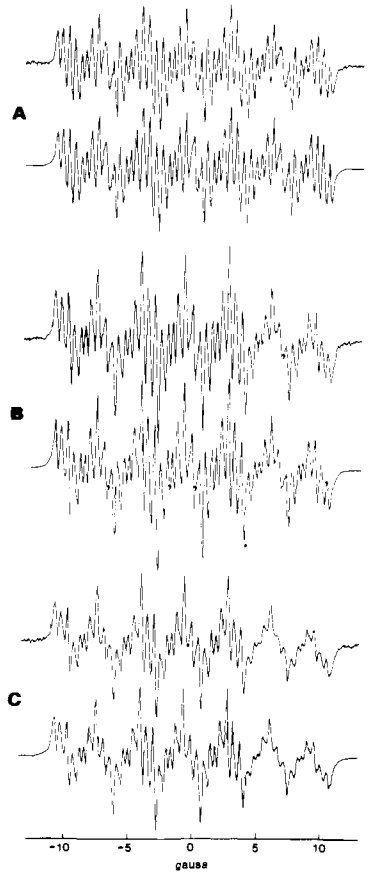


**Figure 4.** EPR spectra of 2-NBA$^{-\cdot}$ in DMF (counterion TBA) at different temperatures. In each case, the upper trace is the experimental spectrum; the lower trace is a matched computer-synthesized spectrum. (A) $T$ = 50 °C; $a_N$ = 6.816 ± 0.001, $a_H$ = 3.450 ± 0.002, $a_H$ = 2.262 ± 0.002, $a_H$ = 0.975 ± 0.003, $a_H$ = 0.527 ± 0.003, $a_H$ = 0.390 ± 0.003, $A$ = 0.242 ± 0.003 G; $R$ = 0.012. (B) $T$ = 0 °C; $a_N$ = 6.815 ± 0.002, $a_H$ = 3.456 ± 0.002, $a_H$ = 2.277 ± 0.002, $a_H$ = 0.964 ± 0.003, $a_H$ = 0.581 ± 0.002, $a_H$ = 0.388 ± 0.003, $A$ = 0.246 ± 0.003, $B_N$ = 0.021 ± 0.002, $C_N$ = 0.041 ± 0.003 G; $R$ = 0.010. (C) $T$ = −20 °C; $a_N$ = 6.795 ± 0.002, $a_H$ = 3.442 ± 0.002, $a_H$ = 2.275 ± 0.002, $a_H$ = 0.951 ± 0.003, $a_H$ = 0.607 ± 0.002, $a_H$ = 0.384 ± 0.002, $A$ = 0.276 ± 0.003, $B_N$ = 0.037, $C_N$ = 0.056 ± 0.004 G; $R$ = 0.009.

Table V. Experimental and Calculated Energetic Results (kcal mol$^{-1}$) for Rotational Isomerizm of Some Benzaldehydes and Their Anion Radicals

| | | molecule | | anion radical | |
|---|---|---|---|---|---|
| benzaldehyde | exptl | exptl | ab initio SCF-MO | exptl | ab initio SCF-MO |
| unsubstituted | $\Delta G^{\ddagger}$ [a] | 7.6,[b] 7.9,[c] 7.7[d] | | | |
| | $\Delta H^{\ddagger}$ | 8.3[d] | 5.93[e] | | 34.71 |
| 4-$NO_2$ | $\Delta G^{\ddagger}$ | 6.6,[f] 6.0[g] | | | |
| | $\Delta H^{\ddagger}$ | | 5.60 | 12.1[h] | 11.78 |
| 3-$NO_2$[k] | $\Delta G^{\ddagger}$ | 7.8–7.1[i] | | 9.35 | |
| | $\Delta H^{\ddagger}$ | | 5.72 | 3.91 | 25.38 |
| | $\Delta G^{\circ}$ | | | 0.98 | |
| | $\Delta H^{\circ}$ | | −0.29 | −1.13 | −1.37 |

[a] Free energies of activation at the coalescence temperature. [b] Reference 31. [c] Reference 32. [d] Reference 33. [e] In ref 34, the use of a slightly different geometry yielded a barrier of 6.6 kcal mol$^{-1}$. [f] Estimated from the experimental barrier of 4-nitroacetophenone (4.4 kcal mol$^{-1}$)[4b] plus the difference between the experimental barriers of benzaldehyde (7.6 kcal mol$^{-1}$)[31] and acetophenone (5.4 kcal mol$^{-1}$).[4b] [g] Estimated from the experimental barrier of 4-nitroacetophenone,[4b] assuming $\sigma$ correlation; $\sigma_p(CHO)/\sigma_p(COCH_3)$ = 1.36 from ref 35. [h] Estimated from the experimental barrier of 4-nitroacetophenone anion radical (8.9 kcal mol$^{-1}$),[2] assuming a $\sigma$ correlation. [k] Signs of energy differences refer to the conversion from the cis isomer to the trans isomer. [i] Estimated from the barrier of 4-nitrobenzaldehyde, assuming a $\sigma$ correlation; $\sigma_m(NO_2)/\sigma_p(NO_2)$ = 1.18 from ref 9.

Table VI. Linear Dependence of Hfs Constants on Temperature for Nitrobenzaldehyde Anion Radicals

| compd | ring position | intercept, G | temp coeff, $10^4$ G K$^{-1}$ |
|---|---|---|---|
| 3-NBA[a] | 2 | 3.128 ± 0.018 | −6.4 ± 0.6 |
| | 3 | 8.643 ± 0.001 | −4.6 ± 0.5 |
| | 4 | 3.955 ± 0.012 | −1.0 ± 0.4 |
| | 5 | 1.131 ± 0.008 | −0.9 ± 0.3 |
| | 6 | 4.594 ± 0.013 | 1.9 ± 0.4 |
| 3-NBA[b] | 2 | 3.013 ± 0.018 | 0.7 ± 0.5 |
| | 3 | 8.344 ± 0.051[c] | 20.4 ± 1.8 |
| | | 5.416 ± 0.187[d] | 108.7 ± 5.4 |
| | 4 | 4.381 ± 0.045[c] | −11.0 ± 1.6 |
| | | 4.468 ± 0.026[d] | −12.4 ± 0.7 |
| | 5 | 1.184 ± 0.014 | −1.0 ± 0.5 |
| | 6 | 5.222 ± 0.022[c] | −15.0 ± 0.8 |
| | | 5.317 ± 0.022[d] | −16.8 ± 0.6 |
| 4-NBA[a] | 1 | 1.336 ± 0.007 | 1.1 ± 0.2 |
| | 2 | 0.345 ± 0.005 | −3.7 ± 0.2 |
| | 3 | 2.462 ± 0.006 | −6.7 ± 0.2 |
| | 4 | 5.604 ± 0.009 | −16.0 ± 0.3 |
| | 5 | 3.227 ± 0.007 | −9.3 ± 0.2 |
| | 6 | 0.457 ± 0.007 | −2.5 ± 0.2 |
| 2-NBA[a] | 1 | 0.855 ± 0.010 | 3.8 ± 0.3 |
| | 2 | 6.732 ± 0.011 | 2.5 ± 0.4 |
| | 3 | 2.320 ± 0.005 | −1.8 ± 0.2 |
| | 4 | 0.360 ± 0.002 | 0.9 ± 0.1 |
| | 5 | 3.414 ± 0.003 | 1.1 ± 0.1 |
| | 6 | 0.901 ± 0.010 | −1.2 ± 0.4 |
| 2-NBA[e] | 1 | 0.980 ± 0.042 | 3.6 ± 1.9 |
| | 2 | 7.176 ± 0.082 | 69.4 ± 3.7 |
| | 3 | 2.532 ± 0.018 | 10.5 ± 0.8 |
| | 4 | 0.735 ± 0.043 | −21.2 ± 2.1 |
| | 5 | 3.460 ± 0.026 | 6.2 ± 1.2 |
| | 6 | 0.435 ± 0.030 | 15.2 ± 1.5 |
| | Na | −0.032 ± 0.015 | 13.2 ± 0.7 |

[a] Electrolytic reduction in DMF containing 0.1 TBAP as a supporting electrolyte. [b] Chemical reduction by $CH_3ONa$ in DMF. [c] Between −5 and 25 °C. [d] Between 60 and 90 °C. [e] Chemical reduction by Na in THF.

the rotation isomers are clearly observable. At higher temperatures averaged spectra are seen, whose hyperfine patterns can be analyzed in terms of averaged hfs constants:

$$\bar{a} = a_c w_c + a_t w_t \quad (4)$$

where $a_c$ and $a_t$ are the hfs constants of the cis and trans forms, respectively, and $w_c$ and $w_t$ are the corresponding equilibrium populations. The hfs constants obtained from a detailed analysis of the spectra at 25 and −50 °C are given in Table I, with the assignments both of the positions in the isomers and to the isomers, based on experimental evidence and qualitative agreement with MO calculations (vide infra). It appears that the spectrum of the cis isomer is more intense than that of the trans one ($w_c/w_t$ = 3.54 at −50 °C). In the whole range of the explored temperatures, the EPR spectra exhibit a slight, though regular, dependence of the hfs constants on temperature. The least-squares fitting of the experimental hfs to a linear model yielded the temperature coefficients collected in Table VI.

In the fast motional region, the contribution of any modulation process to the line widths is described by eq 1–3. The set of line-width parameters ($A$, $B_\alpha$, $C_\alpha$, $E_{\alpha\beta}$, $F_{\alpha\beta}$) can be obtained directly from the experimental spectra through the iterative nonlinear least-squares line-shape fitting method described in the Experimental Section. At all temperatures at which eq 3 holds, a Student's $t$ test and standard deviations on the parameters $B_\alpha$, $C_\alpha$, and $E_{\alpha\beta}$ indicate that their values do not differ from zero significantly. Therefore, the EPR spectra of 3-NBA anion radical in the fast motional region can be analyzed by considering the following line-width expression:

$$W_\lambda = A + (1/4)\sum_{\alpha}^{\text{protons}} F_{\alpha\alpha} + F_{NN}M_{\lambda N}{}^2 + \sum_{\alpha<\beta}^{\text{protons}} F_{\alpha\beta}M_{\lambda\alpha}M_{\lambda\beta} \quad (5)$$

It appears that only the parameters $W_0 = A + (1/4)\sum_{\alpha}^{\text{proton}} F_{\alpha\alpha}$,

Table VII. Kinetic and Thermodynamic Data[a] for the Rotational Isomerizm of 3-NBA$^{-\cdot}$ in DMF (Counterion TBA)

| temp, °C | $10^{-7}k_{obsd}$,[b] $s^{-1}$ | $10^{-6}k_{tc}$,[c] $s^{-1}$ | $10^{-5}k_{ct}$,[d] $s^{-1}$ | $K$[e] |
|---|---|---|---|---|
| 105 | 45 ± 5 | 35 ± 6 | 39 ± 8 | 0.11 ± 0.01 |
| 100 | 38 ± 4 | 32 ± 5 | 38 ± 7 | 0.12 ± 0.01 |
| 90 | 29 ± 2 | 27 ± 3 | 39 ± 3 | 0.14 ± 0.01 |
| 80 | 23 ± 2 | 22 ± 3 | 30 ± 5 | 0.14 ± 0.01 |
| 70 | 17.8 ± 0.8 | 17 ± 2 | 25 ± 3 | 0.14 ± 0.01 |
| 65 | 16.1 ± 0.7 | 17 ± 2 | 29 ± 4 | 0.17 ± 0.01 |
| 60 | 12.8 ± 0.5 | 13 ± 1 | 20 ± 3 | 0.16 ± 0.01 |
| 55 | 10.2 ± 0.3 | 11.3 ± 0.9 | 21 ± 2 | 0.18 ± 0.02 |
| 45 | 9.8 ± 0.3 | 10.6 ± 0.9 | 19 ± 2 | 0.18 ± 0.02 |
| 35 | 4.9 ± 0.1 | 5.3 ± 0.4 | 9 ± 1 | 0.17 ± 0.01 |
| 25 | 4.0 ± 0.1 | 4.6 ± 0.4 | 9 ± 1 | 0.19 ± 0.02 |
| 15 | 2.77 ± 0.06 | 3.4 ± 0.2 | 7.7 ± 0.8 | 0.23 ± 0.02 |
| 10 | 2.08 ± 0.05 | 2.6 ± 0.2 | 6.2 ± 0.7 | 0.24 ± 0.02 |
| 5 | 1.80 ± 0.05 | 2.2 ± 0.2 | 4.7 ± 0.6 | 0.22 ± 0.02 |
| 0 | 1.43 ± 0.05 | 1.7 ± 0.2 | 3.8 ± 0.6 | 0.22 ± 0.02 |
| −5 | 1.23 ± 0.06 | 1.5 ± 0.2 | 3.5 ± 0.6 | 0.23 ± 0.03 |
| −30 | | | | 0.27 ± 0.03 |
| −35 | | | | 0.28 ± 0.03 |
| −40 | | | | 0.31 ± 0.03 |
| −45 | | | | 0.34 ± 0.04 |
| −50 | | | | 0.39 ± 0.03 |
| $\Delta G^{\ddagger}_{298}$ | 7.08 ± 0.01 | 8.37 ± 0.05 | 9.35 ± 0.08 | $\Delta G^{\circ}_{298}$ 0.98 ± 0.06 |
| $\Delta H^{\ddagger}$ | 6.01 ± 0.01 | 5.30 ± 0.02 | 3.91 ± 0.05 | $\Delta H^{\circ}$ −1.13 ± 0.06 |
| $\Delta S^{\ddagger}$ | −3.63 ± 0.02 | −10.30 ± 0.06 | −18.16 ± 0.15 | $\Delta S^{\circ}$ −7.10 ± 0.22 |

[a] Free energies and enthalpies in kcal $mol^{-1}$; entropies in cal $mol^{-1}$ $K^{-1}$. [b] From eq 8. [c] From eq 10. [d] From eq 11. [e] In the fast motional region ($T \geq -5$ °C), from eq 9; in the static region ($T \leq -30$ °C), directly from the experimental spectra as the ratio of the populations of the two rotation isomers.

$F_{NN}$, and the off-diagonal elements of matrix **F** can be determined independently from the experimental spectra.[36] Their values are collected in Table III.

It should be noted incidentally that the signs of the off-diagonal elements of matrix **F** allow us to assign in a natural way the hfs constant of 2.9 G to the proton in position 2. Indeed, it is the only proton hfs constant which is in-phase modulated with the nitrogen hfs constant. The lowest hfs constant (1.1 G) should be located at position 5, as its value is typical of protons in the metal position to a nitro group.[7,9,14] The remaining hfs constants have been assigned to the 4 and 6 protons, specifically (see Table I) on comparison with the hfs constants of 3-nitrobenzamide[11] and 3-nitropyridine[9] anion radicals. Both McLachlan and INDO calculations confirm our assignments.

### Kinetics and Thermodynamics of Internal Rotation

If the potential barrier is sufficiently high so that the radical spends most of the time near the torsional potential minima, the internal rotation can be treated as a chemical exchange between the two possible rotation isomers, according to eq 6. In this case,

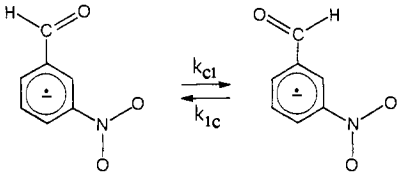


(6)

the parameters $F_{\alpha\beta}$ are given by eq 7, where $\Delta a_\alpha = a_{c,\alpha} - a_{1,\alpha}$ is

$$F_{\alpha\beta} = 2.3^{-1/2}|\gamma_e|\Delta a_\alpha \Delta a_\beta k_{c1}k_{1c}(k_{1c} + k_{c1})^{-3} \quad (7)$$

the difference between the hfs constants of the $\alpha$th nucleus in the two rotation isomers. As the $\Delta a$ values are known from the low-temperature spectra ("static" on the EPR time scale), the pseudo-first-order rate constant

$$k_{obsd} = k_{1c}^{-1}k_{c1}^{-1}(k_{c1} + k_{1c})^3 = 2.3^{-1/2}|\gamma_e|\Delta a_\alpha \Delta a_\beta F_{\alpha\beta}^{-1} \quad (8)$$

(35) Bowers, K. W. In "Radical Ions"; Kaiser, E. T., Kevan, L., Eds.; Interscience: New York, 1968.

(36) For a two-site model, eq 7 holds. Therefore, the five diagonal elements of matrix **F** can be easily obtained from the ten off-diagonal elements by the relationship: $F_{\alpha\alpha} = F_{\alpha\beta}F_{\alpha\gamma}/F_{\beta\gamma}$.

Table VIII. Activation Energies of the Rates of the Rotational Diffusion Process[a]

| compound | solvent | $-E_\eta$, kcal $mol^{-1}$ |
|---|---|---|
| 2-NBA$^{-\cdot}$ $TBA^+$ | DMF | 3.4 ± 0.1 |
| 4-NBA$^{-\cdot}$ $TBA^+$ | DMF | 3.3 ± 0.2 |
| 3-NBA$^{-\cdot}$ $Na^+$ | DMF | 3.3 ± 0.3 |
| 3-NBA$^{-\cdot}$ $TBA^+$ | DMF | 3.2 ± 0.3 |
| 3,5-DNBA$^{-\cdot}$ $TBA^+$[b] | DMF | 3.1 ± 0.2 |
| | DMF[c,d] | 2.0 |
| 2-NBA$^{-\cdot}$$Na^+$ | THF | 2.5 ± 0.1 |
| 3,5-DNBA$^{-\cdot}$$Na^+$[b] | THF | 2.4 ± 0.2 |
| | THF[c,e] | 1.8 |

[a] Average value of the slopes of ln ($B_N T$) vs. $1/T$ and ln ($C_N T$) vs. $1/T$. [b] 3,5-Dinitrobenzamide anion radical, from ref 10. [c] From the slope of $-\ln \eta$ vs. $1/T$, where $\eta$ is the hydrodynamic viscosity of the solvent. [d] From ref 47. [e] From ref 48.

can be readily obtained from eq 7. Although $k_{obsd}$ does not depend on indexes $\alpha$ and $\beta$ explicitly, we may obtain as many $k_{obsd}$ values as there are $F_{\alpha\beta}$'s. The weight-averaged values derived therefrom are reported in the first column in Table VII. The rate constant $k_{obsd}$ gives, at the most, an overall description of the hindered rotation of the formyl group, as it depends on the rate constants of both cis-to-trans and trans-to-cis conversions. As a consequence, interpretation of the activation parameters derived therefrom (cf. Figure 5B and Table VII) is problematic.

To get more insight into the mechanism of hindered rotation, we should combine equilibrium and rate data. Be rearranging eq 4, we obtain the following expression of the equilibrium constant for the cis-to-trans conversion:

$$K = (a_c - \bar{a})(a - \bar{a}_1)^{-1} \quad (9)$$

where $K = k_{c1}/k_{1c} = w_1/w_c$. As noted above, eq 9 holds in the fast motional region where time-averaged EPR spectra are observed. In the "static" region $K$ values can be obtained directly from the experimental spectra as the ratio of the populations of the two rotation isomers. Application of eq 9 requires some knowledge of the dependence of the hfs constants of the two rotation isomers on temperature. As a rule, one should extrapolate the required values of $a_c$ and $a_1$ from their values in the "static" region. In the case of 3-NBA$^{-\cdot}$ only a few data are available from the "static" region, with a general scatter which makes any extrapolation procedure toward higher temperatures somewhat

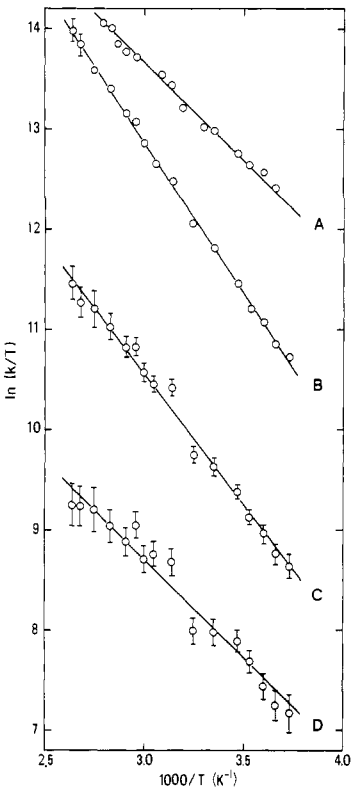


**Figure 5.** Eyring plots of the rate data of internal rotation for 3-NBA in DMF: (A) $k_{obsd}$ (scale shifted by +1.0), correlation factor $r = 0.980$; counterion $Na^+$; (B) $k_{obsd}$, $r = 0.997$, counterion TBA; (C) $k_{tc}$, $r = 0.990$, counterion TBA; (D) $k_{ct}$, $r = 0.932$, counterion TBA.

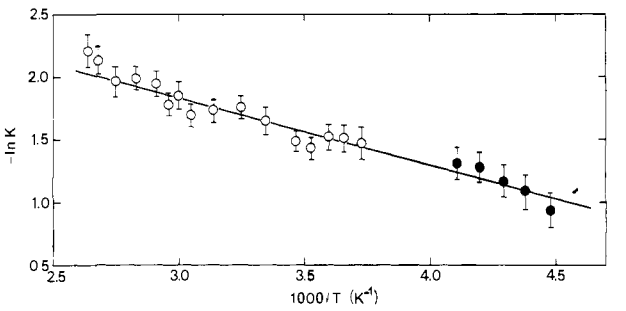


**Figure 6.** van't Hoff plot for the cis ⇄ trans equilibrium of 3-NBA$^{-\cdot}$ in DMF (counterion TBA). In the fast motional region (open circles) $K$ values were evaluated through eq 9. In the "static" region (blackened circles) $K$ values were obtained directly from the experimental spectra as the ratio of the populations of the two rotation isomers. Correlation factor is 0.971.

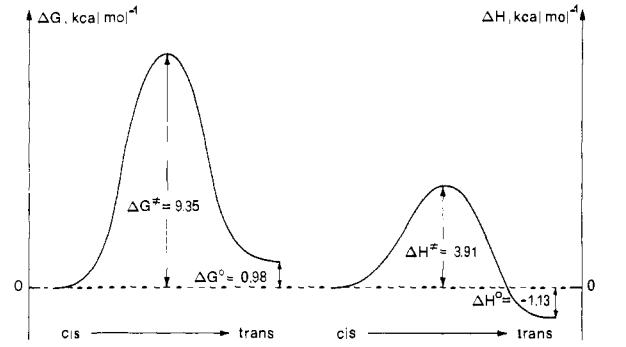


**Figure 7.** Schematic representation of the torsional energy profiles for the 3-NBA anion radical in DMF (counterion TBA).

unsafe. Therefore, $a_c$ and $a_t$ were assumed to be independent on temperature variations; that is, the dependence on temperature of $\bar{a}$ was completely ascribed to the hindered rotation of the formyl group. Application of eq 9 to the nitrogen hfs constant yielded the values collected in the last column of Table VII. These data were fitted to the usual van't Hoff equation, as shown in Figure 6. The corresponding thermodynamic parameters are reported in Table VII. It should be noted that the $K$ values obtained by applying eq 9 to the nitrogen hfs constant correlate quite well (see Table VII and Figure 6) with the $K$ values obtained directly from the "static" EPR spectra at the lowest explored temperatures.[37] This fact substantiates our previous assumption that $da_c/dT \simeq da_t/dT \simeq 0$. Once the equilibrium constant $K$ is known, the rate constants $k_{tc}$ and $k_{ct}$ can be obtained straight through eq 10 and

$$k_{tc} = k_{obsd}K(1 + K)^{-3} \quad (10)$$

11. Their values at different temperatures and the thermodynamic

$$k_{ct} = k_{tc}K \quad (11)$$

constants of the activated complex are collected in Table VII. The corresponding Eyring plots are shown in Figures 5C and 5D.

A complete picture of the energies involved in the internal rotation of the formyl group of 3-NBA anion radical is now available. A schematic representation of the torsional energy profiles is given in Figure 7. It appears from the free-energy profile that the cis isomer is 0.98 kcal mol$^{-1}$ more stable than the trans isomer and that the barrier for the cis-to-trans conversion is 9.35 kcal mol$^{-1}$. On the other hand, the enthalpy profile indicates that the trans isomer is 1.13 kcal mol$^{-1}$ less energetic than the cis isomer. Ab initio UHF-SCF-MO calculations (cf. Table V) gave 1.37 kcal mol$^{-1}$, favoring the trans isomer of 3-NBA anion radical, in good agreement with the experimental enthalpy difference. It is recognized that ab initio MO calculations of conformer energy will, at best, approach the internal energy, or the enthalpy, of an equilibrium geometry, whereas the observed relative conformer populations are determined not by internal energy differences, but by the free-energy differences.[38] However, ab initio calculations strongly overestimate the enthalpy barrier to internal rotation (calcd 25.4, exptl 3.9 kcal mol$^{-1}$). The enthalpy behavior seems due to some intramolecular interactions which decidedly favor the trans form of the 3-NBA anion radical: e.g., (i) the monopolar interaction of the negatively charged oxygen atom of carbonyl group with the negatively charged oxygen atoms of nitro group, (ii) the dipolar interaction between the polar C–O and N–O bonds, and (iii) the repulsion between the lone-pair electrons of the oxygen atoms of the carbonyl group and of the nitro group, respectively.

Comparison of the free energy and enthalpy profiles of Figure 7 points out the relevant entropy contributions to the rotational isomerism of the 3-NBA anion radical. It appears the solvent interactions stabilize the cis form. This result is expected from the reaction field theory of the medium dependence of conformational equilibria. Indeed, the higher nitrogen hfs constant of the trans form favors specific interactions with the surrounding solvent molecules, which yield a positive contribution, $-T\Delta S°$, to the free energy of the cis-to-trans conversion. Activation entropies (see Table VII) indicate that the activated complex is more favorable to efficient solvation and ionic interaction than the ground states. Rotation of the carbonyl group drives both electronic charge and spin density on the nitro group, so that specific solvation of the nitro group, as well complexation of the nitro group by the counterion, is greatly enhanced.

**Solvent Dependence of Internal Rotation.** EPR spectra of 3-NBA$^{-\cdot}$ are markedly affected by solvent properties. both hfs constants and line-width parameters $F$ change regularly with the solvating power of the medium, as shown in Table IV. It appears

(37) Application of eq 9 to the proton hfs constants yielded $K$ values about two times larger, with an enthalpy of about −0.4 kcal mol$^{-1}$. We explain such a discrepancy by reasoning that rotation of formyl group affects the proton hfs constants less than the nitrogen hfs constant, so that the contribution from the internal rotation to the temperature coefficients of proton hfs constants cannot be separated from the contribution of other (e.g., vibronic) mechanisms.

(38) Pullman, B., Ed. "Quantum Mechanics of Molecular Conformations"; Wiley: New York, 1976.

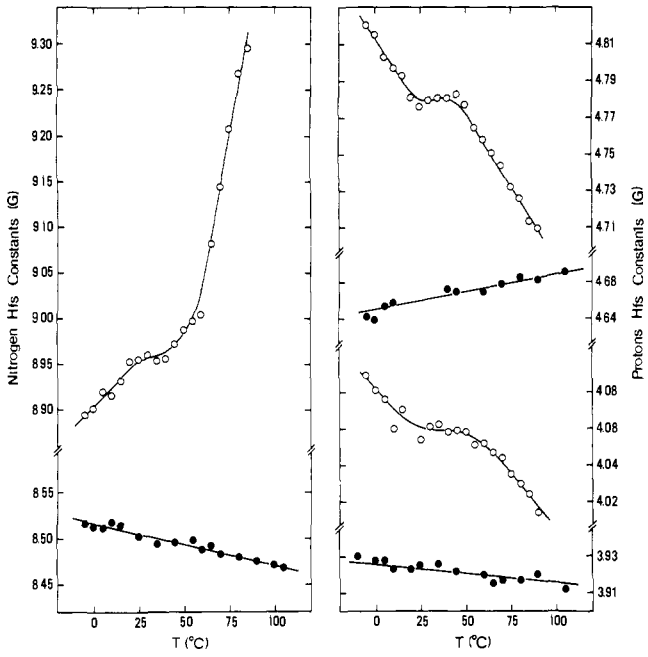


**Figure 8.** Temperature dependence of the averaged hfs constants of 3-NBA$^{-\cdot}$ in DMF. Counterion: Na (open circles), TBA (blackened circles). (Left) Nitrogen, (right) protons hfs constants (upper 6-H, lower 4-H).

that specific solvation occurs at the nitro group more extensively than at the carbonyl group, so that both electronic charge and spin density are further drawn on the nitro group. These facts result in a lower activation energy to internal rotation.

**Ionic Assocation and Internal Rotation.** Probably the most direct way of investigating the effects of ionic associations on internal rotation of the formyl group in 3-NBA$^{-\cdot}$ is to analyze the temperature dependence of the EPR spectra of the corresponding ion pairs with alkali metal cations in ethereal solvents. However, any attempt to obtain the alkali metal ion pairs of 3-NBA$^{-\cdot}$ in tetrahydrofuran and 1,2-dimethoxyethane failed, owing to the high reactivity of 3-NBA in these media. Therefore, we resorted to a study of chemical reduction of 3-NBA with $CH_3ONa$ in DMF; the corresponding EPR spectra were recorded between −50 and +90 °C. By comparing these spectra with those obtained by electrolytic reduction in the same solvent, the following significant changes were observed. (i) The hfs constants increase 2–5% and display a marked dependence on temperature, as shown in Figure 8 and Table VI; their plots vs. $T$ are linear between −5 and +25 °C and between +60 and +90 °C, showing an inflection between +30 and +55 °C. Furthermore, the temperature coefficients of the nitrogen and of 2,6 protons hfs constants reverse their sign. (ii) The logarithmic plots of parameters $F_{N\alpha}/T$ vs. $1/T$ are not linear, whereas the parameters involving only protons display logarithmic plots which are still linear and parallel.

These facts can be easily ascribed to the formation of ion pairs[39] which exist in rapid equilibrium with the free ions. Figure 8 clearly indicates that the effects of ionic association on the hfs constants largely dominate the effects of cis–trans isomerization.[40] Consequently, we cannot use hfs constants to obtain the equilibrium constants of the cis–trans isomerization by means of eq 9. In this case, we should expect that $a_c$ and $a_t$ change markedly with temperature, because of ion pairing. However, from the "static" spectrum at −50 °C we obtain $K = 0.27$. This result states that the cis isomer is more stable in the system 3-NBA$^{-\cdot}$/DMF/$Na^+$ ($\Delta G^\circ_{223}$ = 0.57 kcal mol$^{-1}$) than in the system 3-NBA$^{-\cdot}$/DMF/$TBA^+$ ($\Delta G^\circ_{223}$ = 0.42 kcal mol$^{-1}$).

To get insight into the kinetic mechanism of cis–trans isomerization, one should first recognize how many types of ionic species are present in solution. From the plots in Figure 8, one could guess that free ions (**1**) are present at temperatures lower than −5 °C, rather highly solvated and solvent-separated ion pairs (**2**) exist between +25 and +60 °C, and little solvated or contact ion pairs (**3**) are favored at temperatures higher than 90 °C. Then, one could solve the kinetic system of eq 12 to get the dynamic

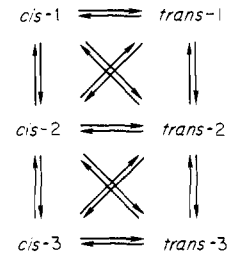


(12)

line-width contributions by means of the procedure outlined in ref 11.

Clearly, the problem has too many unknown (22 rate constants and the hfs constants of each species) so that any fitting procedure cannot be successful. However, a pseudo-first-order kinetic constant can be extracted from the line-width parameters which involve only protons (e.g., $k_{obsd} = (4.8 \pm 0.2) \times 10^7$ s$^{-1}$ at 25 °C).[41] Equation 8 has been used and the corresponding Eyring plot is shown in Figure 5A. The following thermodynamic constants have been derived therefrom: $\Delta G^\ddagger_{298}$ = 6.98 kcal mol$^{-1}$, $\Delta H^\ddagger_{298}$ = 3.89 kcal mol$^{-1}$, and $\Delta S^\ddagger$ = −10.40 cal mol$^{-1}$ K$^{-1}$. It appears that ionic association lowers both the free energy and the enthalpy of activation of the overall process (see Table VII).

**Hindered Rotation of the Formyl Group in 4-NBA$^{-\cdot}$ and 2-NBA$^{-\cdot}$.** We have extended our investigation to the EPR spectra of 4-NBA and 2-NBA anion radicals. Our aim was to establish the effects of both electronic and steric interactions on the internal rotation of the formyl group. 4-NBA$^{-\cdot}$ and 2-NBA$^{-\cdot}$ were obtained by electrolytical reduction in DMF. The spectra of 4-NBA$^{-\cdot}$ were recorded between −40 and +105 °C, those of 2-NBA$^{-\cdot}$ between −40 and +60 °C. 2-NBA was also reduced on sodium mirror in THF, since in this system it yields stable ion pairs. The corresponding spectra were recorded between +14 and −105 °C. The hfs constants of 4-NBA$^{-\cdot}$, 2-NBA$^{-\cdot}$, and 2-NBA$^{-\cdot}$/$Na^+$ display linear dependence on temperature; the corresponding temperature coefficients are collected in Table VI. A few spectra at different temperatures for both 4-NBA$^{-\cdot}$ and 2-NBA$^{-\cdot}$ are reported in Figures 3 and 4, respectively. As previously observed,[3] the EPR spectra of 4-NBA$^{-\cdot}$ shows "coalescence" of the hfs constants of the meta protons at about 60 °C (see Figure 3B). This finding was interpreted[3] in terms of dynamic broadening induced by the internal rotation of the formyl group. Under this assumption, the spectra should be synthesized by the fast motional model[42] at temperatures higher than 60 °C, and by the slow motional model (i.e., the general density matrix method) at temperatures lower than 60 °C.

However, we were able to fit the experimental spectra of 4-NBA$^{-\cdot}$ at all the explored temperatures by means of the static model. The corresponding $R$ factors oscillate between 0.006 and 0.009, which are very good values indeed. Attempts to fit the high-temperature spectra (from 80 to 105 °C) to the fast motional

(39) Substitution of tetra-*n*-butylammonium by sodium cation increases the nitrogen hfs constant by 0.45 G at 25 °C, so that the 3-NBA$^{-\cdot}$/$Na^+$ ion pairs appear to be stronger than the 3-NBA$^{-\cdot}$/$TBA^+$ ion pairs. However, since the sodium quartet is not resolved, we are dealing with "loose" (or solvent-separated) ion pairs or with free ions.

(40) This fact would allow us to obtain the equilibrium constants for the formation of the ion pairs, through the equation: $K_p(Na^+) = (\bar{a} - a_{fl})/(a_{ip} - \bar{a})$ (Alegria, A. E.; Conception, R.; Stevenson, G. R. *J. Phys. Chem.* **1975**, *79*, 361), where $a_{fl}$ and $a_{ip}$ are the hfs constants of the free ion and the ion pair, respectively. Since $a_{fl}$ and $a_{ip}$ are unknown, we cannot obtain reliable values of $K_p$, without introducing arbitrary guesses and approximations.

(41) It is likely that temperature variations of the line-width parameters involving only protons are controlled by internal rotation. Really their values are comparable with the corresponding parameters found for the system 3-NBA$^{-\cdot}$/DMF/$TBA^+$. On the contrary the line-width parameters involving nitrogen contain large contribution from the association process. Such a contribution increases with temperature and at the highest temperatures $F_{NN}$(3-NBA$^{-\cdot}$/DMF/$Na^+$) is found to be about ten times larger than $F_{NN}$(3-NBA$^{-\cdot}$/DMF/$TBA^+$).

model yielded $R$ factors more than three times larger.[43] Therefore, from information provided by our line-shape fitting procedure, it appears that the barrier to internal rotation of the formyl group in 4-NBA$^{-\cdot}$ is too high to be surmounted on an EPR time scale. The observed line-width alternation is accidental in nature and does not depend on any modulation process of isotropic hfs constants. The effective coalescence of the hfs constants modulated by the internal rotation should be expected at temperatures higher than 105 °C. We can estimate a lower limit value for the energy barrier by assuming that the coalescence temperature of the ortho protons hfs constant is at least 110 °C. At the coalescence temperature, the jumping rate of the formyl group is given by[44] $k = 8^{-1/2}|\gamma|\Delta a = 9.3 \times 10^5$ s$^{-1}$. By using the equation[45]

$$k = \pi(E/2J)^{1/2} \exp(-E/RT) \qquad (13)$$

with a reduced moment of inertia $J = 10.49$ amu Å$^2$, the lower limit value $E_{min} = 8.75$ kcal mol$^{-1}$ of the energy barrier is obtained. From this value, the coalescence temperature of meta protons hfs constant is expected to be ≥166 °C in this solvent. Alternatively, the barrier to internal rotation of 4-NBA$^{-\cdot}$ can be estimated from the experimental barrier of 4-nitroacetophenone anion radical (8.9 kcal mol$^{-1}$),[2] assuming a Hammett $\sigma$ correlation. By using $\sigma_p(CHO)/\sigma_p(COCH_3) = 1.36$,[35] we find for 4-NBA$^{-\cdot}$ a barrier of 12.1 kcal mol$^{-1}$, which is in good agreement with the result of the present STO-3G ab initio MO calculation (11.78 kcal mol$^{-1}$).

The EPR spectra of 2-NBA$^{-\cdot}$ and 2-NBA$^{-\cdot}$/Na$^+$ were synthesized by the static model at all the explored temperatures.[46] Only one hfs pattern is observed and, in line with diffractometric results,[28,29] it can be assigned to the trans isomer. Significant steric strains prevent the conversion to the cis isomer, which is moreover destabilized by intramolecular repulsion between the oxygens of the two substituents.

**Transport Properties of Nitrobenzaldehyde Anion Radicals.** EPR spectra of nitrobenzaldehyde anion radicals also display a selective line broadening caused by the modulation of anisotropic (dipolar) components of the nitro group nitrogen hyperfine tensor by rotational Brownian motion[21] of the radicals. This effect has a strong viscosity dependence as expected for dipolar broadening (see, for example, Figure 3C and 4C). According to the rotational diffusion model for the electron spin relaxation in liquids,[21] the line-width coefficients $B_\alpha$ and $C_\alpha$ of eq 2 are proportional to $\eta/T$, where $\eta$ is the viscosity of the solution and $T$ the absolute temperature. As the viscosity $\eta$ follows a Boltzmann distribution,[47,48] the plots of ln $(B_\alpha T)$ and ln $(C_\alpha T)$ vs. $1/T$ are linear and lead to the activation energies reported in Tables VIII. The activation energies of the diffusion process of nitrobenzaldehyde anion radicals in DMF and THF are significantly larger than the solvent hydrodynamic viscosity.[47,48] The observed difference (~1.2 kcal mol$^{-1}$ in DMF) should be representative of the intermolecular potential of the radical anion with the surrounding solvent molecules. Such a difference, if compared with the entropy contribution to the free activation energy of the $k_{obsd}$ process for 3-NBA$^{-\cdot}$ ($-T\Delta S^\ddagger = 1.1$ kcal mol$^{-1}$ at 25 °C), explains the role of the solvent in the mechanism of internal rotation through noticeable entropy contributions.

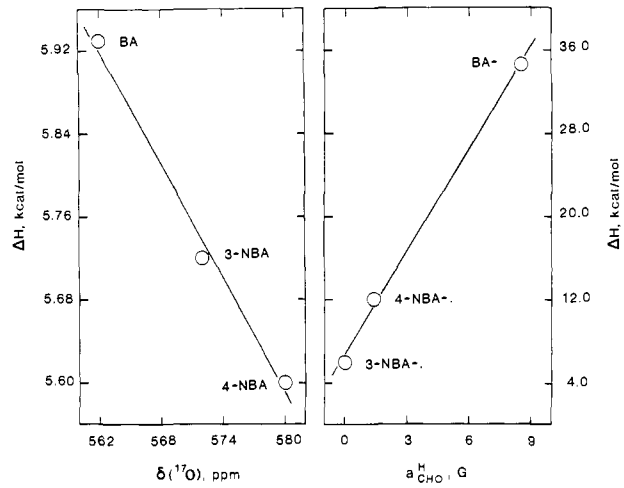


Figure 9. (Left): Mo ab initio STO-3G barriers vs. $^{17}O$ chemical shifts for benzaldehyde and its nitro derivatives. The values for $\delta$ are taken from ref 6. (Right): energy barriers vs. formyl proton hfs constants for benzaldehyde anion radical and its nitrogen derivatives. The ab initio barrier was used for BA$^{-\cdot}$. The values for $a^H_{CHO}$ of BA$^{-\cdot}$ was taken from: Steinberger, N.; Fraenkel, G. K. *J. Chem. Phys.* **1964**, *40*, 723.

## Concluding Remarks and Summary

Detailed analysis of the exchange-broadened EPR spectra of 3-nitrobenzaldehyde anion radical yielded an activation enthalpy of 3.91 kcal mol$^{-1}$ for the conversion of the cis isomer to the trans one. The corresponding isomerization enthalpy amounts to −1.13 kcal mol$^{-1}$. Stabilization of the trans isomer with respect to the cis one is quantitatively predicted ($\Delta H^\ddagger = -1.37$ kcal mol$^{-1}$) by the ab initio MO calculations at the STO-3G level of approximation.

The energy barrier to the internal rotation of the formyl group in the 4-nitrobenzaldehyde anion radical is too high to be surmounted on the EPR scale. At present it may be estimated to be about 12.1 kcal mol$^{-1}$.

By comparing the experimental barriers of the anion radicals with the calculated ones (Tale V), it appears that the value predicted by the MO ab initio STO-3G method for 3-NBA$^{-\cdot}$ is quite unsatisfactory. At this level of approximation, the odd electron is apparently more localized on the benzaldehyde fragment than on the nitrobenzene fragment. It appears that experimental rotational barriers of anion radicals can give direct evidence of the goodness of the wave function for open-shell systems. In view of this, further investigations of the energy barriers of anion radicals should be desirable.

MO ab initio calculations of this level of approximation predict barriers of 5.9, 5.7, and 5.6 kcal mol$^{-1}$ for benzaldehyde and its meta and para nitro derivatives, respectively. This trend can be explained in terms of qualitative MO theories. It should be expected that the electron-withdrawing power of the nitro group decrease the double-bond character of the $C_1$–$C_\alpha$ bond. This fact results in a lower barrier to the internal rotation about that bond. Inductive effects are transmitted with equal effectiveness from both the meta and para positions, whereas resonance effects are most efficiently transmitted from the para position. Thus the lower barrier of 4-NBA is most likely due to mesomeric effects. Clearly canonical structures of the quinoid type, which are not possible for meta compounds, contribute significantly to the ground state of 4-NBA.

On the grounds of these considerations, we can explain the correlation observed (Figure 9) between the calculated barriers of some benzaldehydes and the corresponding $^{17}O$ NMR chemical shifts.[6] As proof, it should be also noted that the barriers to internal rotation decrease as Hammett's $\sigma$ values for the nitro group increase ($\sigma_m(NO_2) = 0.710$; $\sigma_p(NO_2) = 0.778$).[49] In the

(42) The contribution to the line width induced by the out-of phase modulation of the pairs of coupling ($a_{2\text{-H}}$, $a_{6\text{-H}}$) and ($a_{3\text{-H}}$ and $a_{5\text{-H}}$) of 4-NBA$^{-\cdot}$ has the following expression: $W_{exch,\lambda} = F_{ortho}(m_2 - m_6)^2 + F_{meta}(m_3 - m_5)^2 + 2(F_{ortho}F_{meta})^{1/2}(m_2 - m_6)(m_3 - m_5)$. The $F$'s are given by eq 7. However, in the case of 4-NBA$^{-\cdot}$, we are dealing with a mutual exchange between two equivalent sites, so that $K_{obsd} = 8k$.

(43) The values of $F$ parameters depend slightly on temperature, and the corresponding logarithmic plots give an activation energy of 0.96 ± 0.07 kcal mol$^{-1}$. This value is too low to be interpreted as the energy barrier to the internal rotation formyl group of 4-NBA$^{-\cdot}$. This finding further supports the failure of the dynamical model.

(44) Carrington, A.; McLachlan, A. D. "Introduction to Magnetic Resonance"; Harper and Row: New York, 1967.

(45) Das, T. P. *J. Chem. Phys.* **1957**, *27*, 763.

(46) Also the spectra of 2-NBA$^{-\cdot}$ and 2-NBA$^{-\cdot}$/Na$^+$ display an accidental line-width alternation which affects the multiplet of protons 4 and 6 (cf. Figure 4).

(47) Hyde, J. S.; Sarna, T. *J. Chem. Phys.* **1978**, *68*, 4439.

(48) Carvajal, C.; Tolle, K. J.; Smid, J.; Szwarc, M. *J. Am. Chem. Soc.* **1965**, *87*, 5548.

(49) Jaffé, H. *Chem. Rev.* **1953**, *53*, 191.

anion radicals of benzaldehyde and its nitro derivatives, the odd electron is delocalized on an extensive conjugated system. The barrier heights increase accordingly with the double-bond character of the $C_1$–$C_\alpha$ bond,[50] but the increment is greater for benzaldehyde than for 4-NBA and 3-NBA, owing to the electron-withdrawing power of the nitro group. As a consequence, a nice correlation is observed (Figure 9) between the experimental barriers and the hfs constants of the formyl proton. Accordingly, the experimental barriers decrease as the nitro group $\sigma^-$ values increase ($\sigma_p^-(NO_2)$ = 0.828; $\sigma_m^-(NO_2)$ = 0.975).[9]

Solvent interactions and ionic associations make the cis isomer of 3-NBA$^{-\cdot}$ more stable than the trans isomer through noticeable entropy contributions to the free energy of the isomerization process. The free energy of activation of the internal rotation decreases as the solvating power of the solvent or the strength of ionic association increases. Analysis of the diffusional process of the anion radicals in solution has provided direct evidence of specific interactions between the anion radicals and the surrounding solvent molecules.

(50) The Mulliken reduced overlap populations (Mulliken, R. S. *J. Chem. Phys.* **1955**, *23*, 1833, 1841, 2338, 2345) for the $C_1$–$C_\alpha$ bond, calculated from the MO ab initio STO-3G wave functions, are 0.380, 0.379, 0.378 for benzaldehyde, 3-NBA, and 4-NBA, and 0.441, 0.393, and 0.399 for the corresponding anion radicals, respectively.

**Registry No.** 3-NBA radical anion, 40951-85-7; 4-NBA radical anion, 34512-33-9; 2-NBA radical anion, 57643-03-5; benzaldehyde, 100-52-7; 4-nitrobenzaldehyde, 555-16-8; 3-nitrobenzaldehyde, 99-61-6; benzaldehyde radical anion, 34473-57-9.

# Investigation of Some Intermolecular Electron Transfer Reactions of Cytochrome *c* by Electrochemical Methods

**H. Allen O. Hill* and Nicholas J. Walton**

*Contribution from the Inorganic Chemistry Laboratory, Oxford OX1 3QR, England.*
*Received December 21, 1981*

**Abstract:** An electrochemical investigation of the reaction of horse heart cyclochrome *c* with the redox proteins from *Pseudomonas aeruginosa*, cytochrome $c_{551}$ and azurin, in the presence of *P. aeruginosa* nitrite reductase/cytochrome oxidase and dioxygen, is described. The electrochemical reduction of horse heart cytochrome *c* is coupled to the reduction of dioxygen via the redox proteins from *P. aeruginosa*; 3.5–3.8 faradays mol$^{-1}$ of dioxygen is consumed.

Electron transfer between proteins is a crucial and essential process in all living organisms. The factors which govern and control these intermolecular reactions and allow rapid electron transfer concomitantly with selectivity and specificity in choice of partners deserve to be elucidated. There have been a number of valuable studies[1-8] which have served to identify some features of protein structure that appear to be important such as the nature and disposition of charged groups on the surface of the protein and the location of the redox center with respect to the surface.

Most electrochemical investigations of redox proteins have made use of small-molecule electrode-active mediators, either bound[9] to the electrode surface or free in solution[10-18] which enhance the rate of electron transfer between electrode and protein. To date, there have been only a few reported[19] cases of *direct* electron transfer to redox proteins, e.g., eukaryotic cytochromes[20,21] *c*, cytochromes[22-25] $c_3$, and ferredoxin.[26,27] Our own contribution[21] has mainly centered on the use of electrodes upon which 4,4′-bipyridyl or related materials are absorbed. The electrochemistry of horse heart cytochrome *c* is well-behaved at such electrodes and we have proposed[21] that the cytochrome adsorbs onto and desorbs from the electrode surface rapidly, the favorable binding interaction being responsible for the enhancement of the rate of the electrode reaction. In this paper we describe the electrochemical investigation of electron transfer reactions of horse heat

(1) Kang, C. H.; Brautigan, D. L.; Osheroff, N.; Margoliash, E. *J. Biol. Chem.* **1978**, *253*, 6502-10.
(2) Speck, S. H.; Koppenol, W. H.; Dethmers, J. K.; Osheroff, N.; Margoliash, E.; Rajagopalan, K. V. *J. Biol. Chem.* **1981**, *256*, 7394-400.
(3) Cummins, D.; Gray, H. B. *J. Am. Chem. Soc.* **1977**, *99*, 5158-67.
(4) Mauk, A. G.; Scott, R. A.; Gray, H. B. *J. Am. Chem. Soc.* **1980**, *102*, 4360-3.
(5) Kraut, J. *Biochem. Soc. Trans.* **1981**, *9*, 197-202.
(6) Dickerson, R. E.; Takano, T.; Eisenberg, D.; Kallai, O. B.; Samson, L.; Cooper, A.; Margoliash, E. *J. Biol. Chem.* **1971**, *246*, 1511-35.
(7) Almassy, R. J.; Dickerson, R. E. *Proc. Natl. Acad. Sci. U.S.A.* **1978**, *75*, 2674-8.
(8) Adman, E. T.; Jensen, L. H. *Isr. J. Chem.* **1981**, *21*, 8-12.
(9) Lewis, N. S.; Wrighton, M. S. *Science* **1981**, *211*, 944-7.
(10) Feinberg, B. A.; Ryan, M. D.; Wei, J.-F. *Biochem. Biophys. Res. Commun.* **1977**, *79*, 769-75.
(11) Ryan, M. D.; Wei, J.-F.; Feinberg, B. A.; Lau, Y.-K. *Anal. Biochem.* **1979**, *96*, 326-33.
(12) Wei, J.-F.; Ryan, M. D. *Anal. Biochem.* **1980**, *106*, 269-77.
(13) Dasgupta, S.; Ryan, M. D. *Bioelectrochem. Bioenerg.* **1980**, *7*, 587-94.
(14) Hawkridge, F. M.; Kuwana, T. *Anal. Chem.* **1973**, *45*, 1021-7.
(15) Heineman, W. R.; Norris, B. J.; Goelz, J. F. *Anal. Chem.* **1975**, *47*, 79-84.
(16) Ryan, M. D.; Wilson, G. S. *Anal. Chem.* **1975**, *47*, 885-90.
(17) Richard, L. H.; Landrum, H. L.; Hawkridge, F. M. *Bioelectrochem. Bioenerg.* **1978**, *5*, 686-96.
(18) Heineman, W. R.; Meckstroth, M. L.; Norris, B. J.; Su, C.-H. *Bioelectrochem. Bioenerg.* **1979**, *6*, 577-85.
(19) Eddowes, M. J.; Hill, H. A. O. *Biosci. Rep.* **1981**, *1*, 521-32 and references therein.
(20) Yeh, P.; Kuwana, T. *Chem. Lett.* **1977**, 1145-8.
(21) Albery, W. J.; Eddowes, M. J.; Hill, H. A. O.; Hillman, A. R. *J. Am. Chem. Soc.* **1981**, *103*, 3904-10 and references therein.
(22) Niki, K.; Yagi, T.; Inokuchi, H.; Kimura, K. *J. Am. Chem. Soc.* **1979**, *101*, 3335-40.
(23) Sokol, W. F.; Evans, D. H.; Niki, K.; Yagi, T. *J. Electroanal. Chem. Interfacial Electrochem.* **1980**, *108*, 107-15.
(24) Bianco, P.; Faugue, F.; Haladjian, J. *Bioelectrochem. Bioenerg.* **1979**, *6*, 385-91.
(25) Bianco, P.; Haladjian, J. *Electrochim. Acta* **1981**, *26*, 1001-4.
(26) Landrum, H. L.; Salmon, R. T.; Hawkridge, F. M. *J. Am. Chem. Soc.* **1977**, *99*, 3154-8.
(27) Kakutani, T.; Toriyama, K.; Ikeda, T.; Senda, M. *Bull. Chem. Soc. Jpn.* **1980**, *53*, 947-50.

0002-7863/82/1504-6515$01.25/0 